*Original Article*

# Atomic layout of an orthodontic titanium mini-implant in human tissue: *Insights into the possible mechanisms during osseointegration*

**Jun-Sik Kim[a*]; Jae-Pyeong Ahn[b*]; Yang-Hee Kim[c]; Kyung Won Seo[c]; Homayoun Zadeh[d]; Seong-Hun Kim[e]**

**ABSTRACT**

**Objectives:** To evaluate nanoscale molecular interactions in the interface between human bone and orthodontic titanium implants.

**Materials and Methods:** An orthodontic implant (sandblasted with large grit and with an acid-etched surface treated with Ti6A14V alloy) retrieved from the mandible of human after 2 months of healing was used to analyze the molecular interactive mechanism between the implant and the surrounding bone tissue. To preserve the natural state of the sample as much as possible, cryofixation and scanning electron microscope/focused ion beam milling without any chemical treatment were used during sample preparation. Atom probe tomography was used to investigate the chemical composition and structure at the interface between the implant and human bone tissue.

**Results:** Three-dimensional (3D) reconstruction of the whole sample revealed a $20 \times 50$-nm$^2$ plate-like bony element diffusion layer in the sample. The iso concentration analysis of the diffusion layer indicated that the bony element, calcium, and the implant element, titanium oxide, were interspersed with each other. Detailed ionic distribution was illustrated by 3D reconstruction with partial region of interest and one-dimensional concentration profiles of the implant-bone interface.

**Conclusions:** The study results advance nanoscale understanding of osseointegration and suggest a potential nanostructure for increasing bond strength of biomaterials to bone. (*Angle Orthod.* 2019;89:292–298.)

**KEY WORDS:** Osseointegration; Titanium implant; Cryofixation; Atom probe tomography; Implant-bone interface; SLA

## INTRODUCTION

Osseointegration has traditionally been defined as a direct connection formed between a load-carrying implant surface and bone tissue.[1–3] In orthodontic treatment, titanium implants have been used as the source of anchorage since they can resist both rotational force and heavy force due to osseointegration.[4] Surface-treated mini-implants have been used for various orthodontic tooth movements, such as en masse retraction of anterior teeth, distalization of posterior teeth, and intrusion of posterior teeth.[5,6] Several surface modifications and their clinical significance have been evaluated by removal torque, cellular experiments, and bone contact area ratios.[6–8] Although the success and prognosis of an implant depends on the osseointegration between the implant and the surrounding bone,[9] its molecular mechanism remains undetermined until now.

Visualization of biointerfaces on a three-dimensional (3D) molecular level could reveal new fundamental

[a] Postgraduate student, Department of Orthodontics, Graduate School, Kyung Hee University, Seoul, Korea.

[b] Director, Advanced Analysis Center, Korea Institute of Science and Technology, Seoul, Korea.

[c] Research Fellow, Advanced Analysis Center, Korea Institute of Science and Technology, Seoul, Korea.

[d] Associate Professor, Laboratory of Immune Regulation and Tissue Engineering, Herman Ostrow School of Dentistry, University of Southern California, Los Angeles, Calif.

[e] Professor and Head, Department of Orthodontics, Graduate School, Kyung Hee University, Seoul, Korea.

Corresponding author: Dr Seong-Hun Kim, Professor and Head, Department of Orthodontics, Graduate School, Kyung Hee University, Seoul 130-701, Korea
(e-mail: bravortho@khu.ac.kr)

Accepted: October 2018. Submitted: May 2018.
Published Online: November 28, 2018

information on material properties and bone response.[10] Previously, various methods have been used to investigate the bone-titanium (Ti) interface at the macro-, micro-, and nanoscales in an effort to elucidate the mechanism of osseointegration. Light and electron microscopic studies[9,11] have also demonstrated intimate contact between titanium implant surfaces and bone. A recent nanoscale study[9] demonstrated the coexistence of Ti, oxygen (O), calcium (Ca), and phosphorus (P) at a distance of approximately 100 nm from the implant surface, suggesting that bone ingrowth occurs within a titanium oxide (TiO) layer. Other studies[12] showed that direct contact between Ca atoms of bone and the TiO area of implants with different kinds of surface treatment is formed without the presence of a protein interlayer through the use of atom probe tomography with chemical fixation and resin embedding. However, no study has been reported showing the atomic layout of the interface between a sandblasted, large-grit, and acid-etched (SLA)–surface titanium implant and human tissue without chemical pretreatment.

The purpose of the present study was to determine the feasibility of atom probe tomography (APT) analysis on the interface between biomaterial and human tissue in its native state and to investigate the detailed 3D atomic structure of the interface between a SLA surface implant and human bone without chemical pretreatment.

## MATERIALS AND METHODS

The implant was composed of $Ti_6Al_4V$ ELI (extra-low interstitials), as standardized in ASTM-F136-Rev:2 (C-implant, CIMPLANT Co, Seoul, Korea). The specific composition (wt%) was 6.1% aluminum (Al), 3.9% vanadium (V), 0.004% carbon (C), and 0.114% oxygen (O), with the remainder composed of Ti. The surface of the implant was treated by sandblasting with large grit and acid etching to achieve a microtexture. The implant was 1.8 mm in diameter and 8.5 mm in length. The C-implant's characteristics of good osseointegration and easy removal facilitated the present study.[6] The sample was obtained from a 23-year-old-female patient with missing teeth in the lower left second premolar area. The implant was initially planned as orthodontic anchorage for space closure, but the patient later opted for crown and bridge replacement in that area. The C-implant was easily removed using a manual screwdriver without a trephine bur because the interface between the bone and the implant should be located close to the surface in order to prepare samples for nanoscale analysis using scanning electron microscope/focused ion beam (SEM-FIB) without preprocessing such as chemical fixation, resin embedding, and sectioning.[2] This study was performed under approval from the Institutional Review Board of Kyung Hee University Dental Hospital (KMC-IRB-1409-1).

### Preparation of Samples for APT

The retrieved implant was placed in saline solution and sent to the lab for cryofixation in ethane solution within 1 hour of removal. The implant was then gradually dried to room temperature in a vacuum chamber.[13] The SEM/FIB instrument (Helios-Nanolab-600, FEI, Hillsboro, Oreg) operated in backscattering mode was used for ex vivo detection of bone formation around the retrieved implant and APT analysis. Region-of-interest (ROI) marking and protection layer deposition were performed using an E-beam (5 kV, 86 pA). A platinum (FIB-Pt) rectangle was deposited on the polished cross section of specimens using an ion beam (30 kV, 93 pA). A U-shaped wedge of the specimen under the Pt-rectangle was dissected out on three sides using a gallium (Ga) FIB (30 kV, 6.5 nA) to obtain the specific ROI on the Si-post for APT. The dissected wedge was attached to an in situ nanomanipulator (Omniprobe, Dallas, Tex) using FIB-deposited Pt and was then cut free from the final edge of the specimen. Sequential segments (1–2 $\mu$m wide) were cut from the wedge and affixed to the tops of Si-posts in an array (Cameca Scientific Instruments, Madison, Wisc) with FIB-Pt. Each tip was shaped and sharpened using annular milling patterns of increasingly smaller inner and outer diameters. The majority of the amorphized surface region and implanted $Ga^+$ ions on the tip surface were removed by a final low-voltage ion-milling step at 2 kV and 46 pA.

### APT Analysis

The APT analyses were conducted using a local-electrode APT unit (LEAP-4000HR, Cameca). Field evaporation was initiated by pulsing with an Nd:YAG green laser ($\lambda = 355$ nm) while optimizing the run time parameters (160 kHz, 200 pJ/pulse) for hydroxyapatite (OHAp). The base temperature of the microtip was maintained at 64.8 K, and the vacuum pressure was approximately $5.3 \times 10^{-11}$ Torr. The detection rate was 0.3%. Peak ranges were defined as the entire visible peak, and the background was corrected by sideband subtraction. APT data analysis was conducted using Cameca-IVAS3.6.6 software. SEM micrographs of the final tip shape were used to estimate the evolution of the radius of the APT specimen during analyses.

## RESULTS

The sample for APT analysis on the osseointegration was successfully prepared from the retrieved

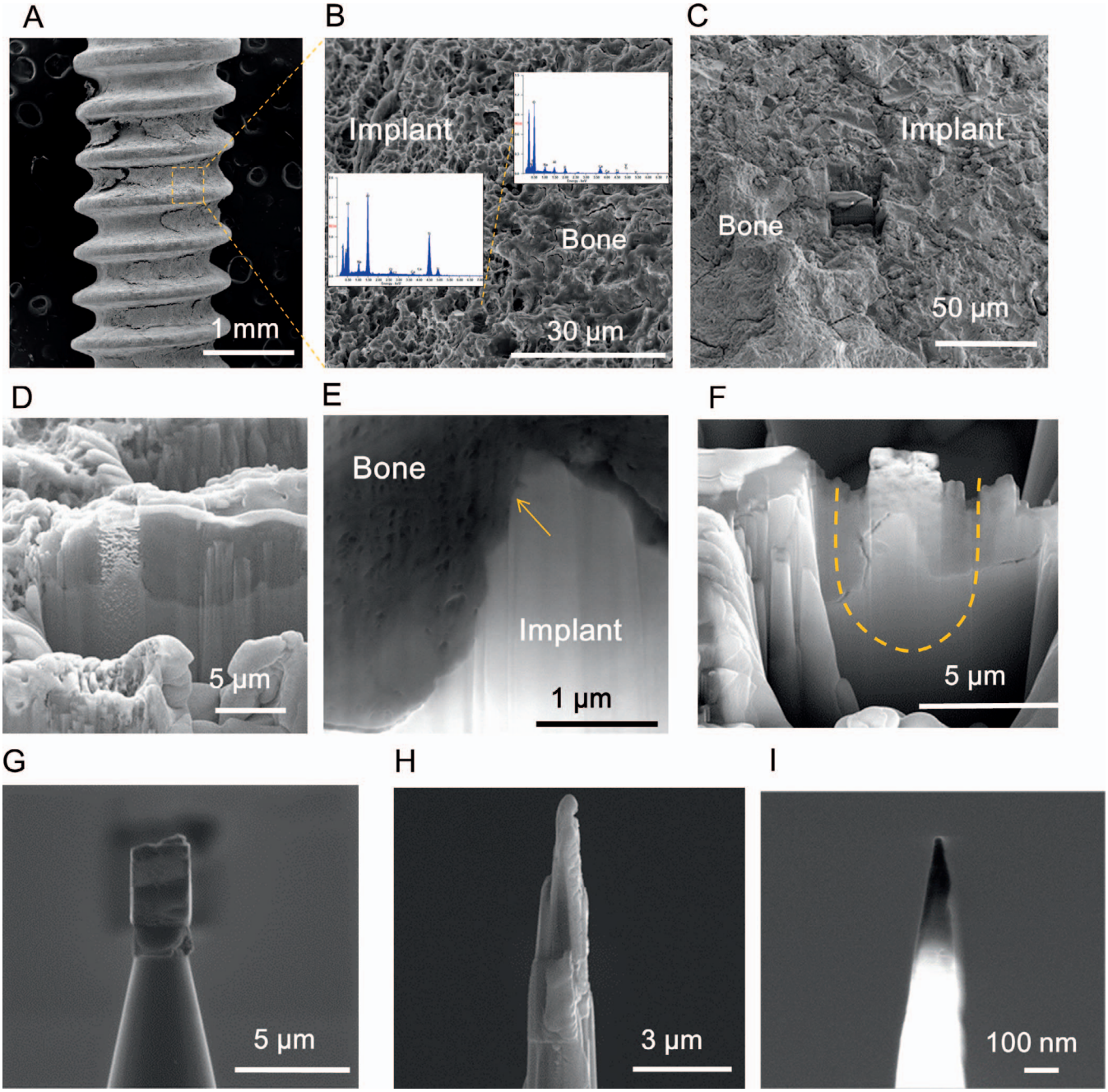


**Figure 1.** Sample preparation for APT analysis. (A) SEM images of the dental mini-implant. (B) SEM image of the mini-implant shows the attachment of bone in some areas. Upon magnification, the bone displays integration with the mesoporous surface of the SLA-treated titanium mini-implant. EDS analysis identified the Ca peak of the major bone component. (C) The bone-to-implant contact area was revealed from the bulk sample by FIB milling. (D) A platinum (FIB-Pt) rectangle was deposited on the polished cross section of specimens. (E) The cross-sectional image between the bone and titanium implant demonstrates tight integration. The arrow represents the bone-implant interface that was lifted out for FIB-sampling. (F) A U-shaped wedge of the specimen under the Pt rectangle was dissected out on three sides, as represented by the dashed line. (G) A segment (2 μm wide) was affixed to the top of the Si post. (H) Tip was shaped and sharpened by annular milling. (I) Final tip shape after low-voltage ion milling.

implant by the SEM/FIB method without chemical fixation, dying, and resin embedding. At first, thin human bone was verified on the cryofixed implant under SEM energy-dispersive x-ray spectroscopy observation (Figure 1A,B). SEM/FIB analysis on the cross section of the specimen showed direct and intimate contact between bone and the implant (Figure 1C–I). Eventually, two samples were obtained for APT analysis with an intact bone-implant contact. Examination of the samples demonstrated that they were

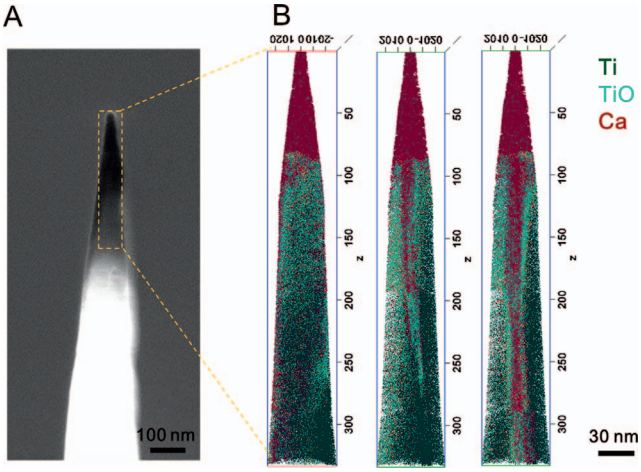


**Figure 2.** The left SEM image shows the atom probe analysis implant sample (probe shaped) prepared through FIB treatment (A). The three images on the right display 3D distribution maps reconstructed using the IVAS program. When the 3D map is shown at different angles, the overall distribution of the constituent atoms can be identified (dark green, titanium; light green, titanium oxide; brown, calcium) (B).

suitable for APT analysis because the intact bone-implant interface was placed within the 50–100-nm diameter (Figure 2A). When the samples were divided into bone, implant, and interface for peak indexing, the ionic configurations were well matched to the assumed values for each part. The mass spectrum of the bone exactly matched the known APT mass spectrum of bone-type mineralized tissue,[14] confirming validity of the method.

## APT Analysis With the Whole Sample

3D reconstruction of the whole sample (Figure 2B) showed that the top 50-nm section of the sample was composed solely of bone. In the middle layer, there was a 20 × 50-nm$^2$ plate-like diffusion layer with bony elements in the longitudinal direction. Pure Ti alloys were present on both sides of the diffusion layer. Abundant hydrogen specifically coexisted in this implant area, pure Ti alloy layer. An extensive amount of TiO was observed throughout the remainder of the sample, except in the top layer of the bone and implant area. The iso-concentration analysis and one-dimensional (1D) profile analysis indicated that Ca was abundant throughout the bone, as Ca was present in reduced amounts through the middle diffusion area, and no Ca was observed in the implant. Conversely, Ti was found mostly throughout the implant, with reduced levels in the diffusion area, and was not observed in the bone. P, potassium (K), and C showed similar distributions to that of Ca. TiO was not observed in the bone and was scarce in the implant but was prevalent in the middle diffusion area. Oxidized aluminum (AlO) and oxidized vanadium (VO) showed similar distributions to TiO.

## APT Analysis With Partial ROI

To avoid peak overlaps, five sections with 5 × 5 × 80-nm$^3$ ROI about all layers (bone, interface, and implant) were made and surveyed using the high-resolution IVAS program. The top bone layer (area A in Figure 3; Table 1) showed abundant Ca, P, C, O, and

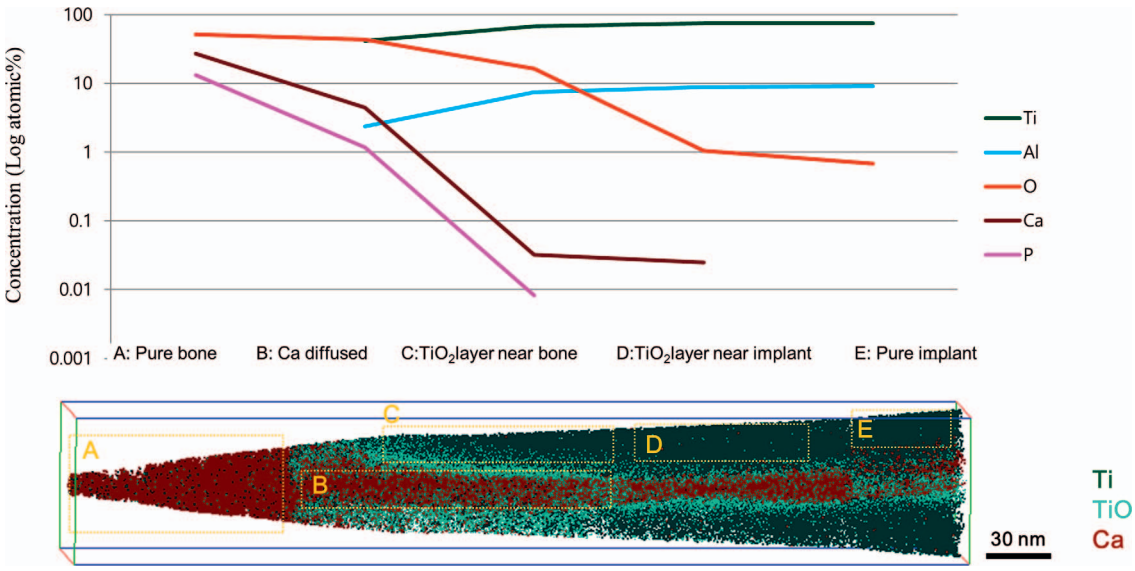


**Figure 3.** The overall changes in the atomic composition of the sample within five discrete zones. Each of these zones was individually analyzed as a region of interest, namely: bone (A, pure bone), bone-implant interface (B, Ca-diffused region); C, titanium-dioxide layer adjacent to bone; D, oxidized Ti near implant), and implant (E, pure implant). The Ti, Al, O, Ca, and P contents in each area were analyzed quantitatively.

**Table 1.** Quantitative Analysis of the Overall Changes in the Atomic Composition of the Sample from A to E (Figure 3)[a]

| | ROI | Ti | Al | V | O | Ca | P | C | H | K | N | Cl | Total |
|---|---|---|---|---|---|---|---|---|---|---|---|---|---|
| A | Pure bone | 0 | 0 | 0 | 44.1961 | 39.1428 | 10.9502 | 3.9414 | 1.3525 | 0 | 0.417 | 0 | 100 |
| B | New bone | 41.5937 | 2.3681 | 0.9127 | 43.3403 | 4.4609 | 1.1707 | 1.0976 | 4.4774 | 0.2614 | 0.1357 | 0.1815 | 100 |
| C | O-Ti near bone | 67.5219 | 7.4265 | 2.3301 | 16.369 | 0.0323 | 0.0082 | 0.1124 | 6.1216 | 0 | 0.0635 | 0.0144 | 99.9999 |
| D | O-Ti near Ti | 75.2781 | 8.8894 | 2.3722 | 1.0534 | 0.0248 | 0 | 0.0115 | 12.3605 | 0 | 0 | 0 | 99.9899 |
| E | Pure Ti | 75.5035 | 9.118 | 2.4428 | 0.6775 | 0 | 0 | 0 | 12.2582 | 0 | 0 | 0 | 100 |

[a] ROI indicates region of interest; Ti, titanium; Al, aluminum; V, vanadium; O, oxygen; Ca, calcium; P, phosphorus; C, carbon; H, hydrogen; and K, potassium.

hydrogen (H) ions, with no implant components. The exceptionally high Ti density, which was identified with whole-spectrum indexing in the bone area, likely resulted from the Ca peak-tail in the Ti section of the spectrum. In the separate spectrum of the bone area only, there was no Ti indexing. In the interface (areas B, C, and D in Figure 3), there was a gradual increase of TiO from the implant to the interface. On the contrary, Ca and P existed with TiO at the interface, and their concentrations decreased toward the implant. This was in agreement with the results of conventional studies.[2,9]

The 1D profile of the Ca diffused layer (area B in Figure 3) showed the coexistence of Ca, P, C, O, and TiO. A markedly high Ca content was observed in the diffusion layer near the bone. CO was found in the top interface layer. The implant area (area E in Figure 3) contained Ti, Al, V, and H, and no bone components were present. The ratio of Ca and P in the bone area was identical to that of natural bone tissue. In the interface (areas B, C, and D in Figure 3), Ti and P peaks overlapped, which hindered accurate analysis of the distribution of P. In the pure bone (area A in Figure 3) without overlapped peak, the distribution of P was similar to that of Ca. Also, a copious amount of H was present throughout the sample.

### 3D Reconstruction and 1D Concentration Profiles of the Implant-Bone Interface

In the 3D reconfiguration map, the interface from the implant toward the bone formed as a diffused oxygen layer, AlO layer, TiO layer, and Ca-diffused layer (Figure 4A). The 1D profile with area around 50% isosurface of Ti showed that Ca, CaAlO, and CaVO ions were scarce in this area (Figure 4B). In the iso surface analysis, the TiO in the interface appeared as fleecy clouds. Ca showed a similar pattern, which could mean that Ca and TiO were interspersed at the interface (Figure 4A). 1D profiling showed that the oxygen content decreased from the interface toward the implant (Figure 4B). Oxygen was present in the form of calcium phosphate in the bone, whereas it was present as TiO, AlO, and VO at the interface. In the 1D profile, the Ca concentration decreased toward the

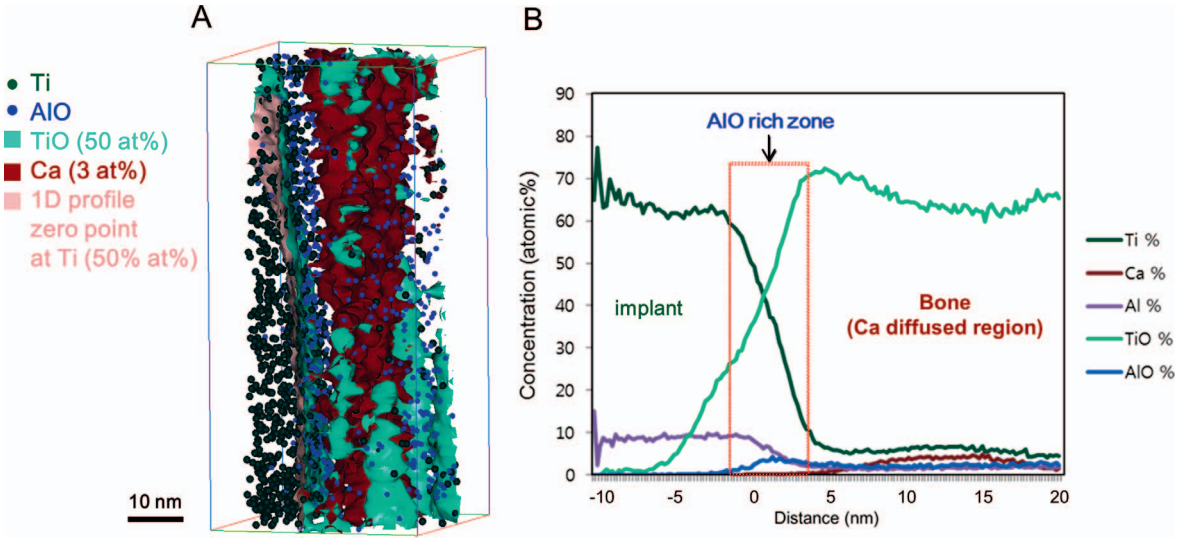


**Figure 4.** 3D reconstruction and concentration analysis of the bone-implant interface. (A) 3D reconstruction image showing Ca diffusion within the titanium oxide layer, as well as titanium oxide within the bone region, confirming the intermingling of Ca and TiO2 atoms. Iso-concentration surfaces of TiO (light green) and Ca (brown) are displayed along with individual $Al_2O_3$ (blue) and Ti (dark green) atoms. (B) 2D profile of the major atoms (the pink iso-concentration surface highlights the distance zero area). An $Al_2O_3$-rich area with four times the normal concentration is observed between Ti and $TiO_2$.

implant; Ca penetrated 8–10 nm into the implant, but the presence of a 4-nm-wide layer of AlO prevented further penetration, even with TiO (Figure 4B).

## DISCUSSION

Previous studies[3,9] used the retrieved implant and surrounding bone, which were chemically fixed, dehydrated, embedded in plastic resin, and then longitudinally cut and polished according to the protocol proposed by Taborelli et al.[15] However, these chemical pretreatments could increase the risk of sample contamination and distortion.[13] Pretreatment could lead to possible loss or distortion of key attributes of nanoscale osseointegration. In order to bypass these chemical pretreatments of the samples, they were prepared by cryofixation and sliced using the in situ SEM/FIB protocols for APT analysis in the present study.

When the molecular information of a material is studied, the preparation method should preserve not only the morphological structure of the sample but also its native chemical composition. As described in previous articles,[13,16] a preparation protocol involving cryofixation and subsequent freeze drying can be used for preparing well-preserved cell samples for TOF-SIMS (Time-of-Flight Secondary Ion Mass Spectrometry) and APT-analysis. Malm et al.[16] reported that cryofixation by plunge freezing in liquid propane offered superior capacity in terms of preserving the chemical composition of cells when compared to chemical fixation by glutaraldehyde. Meanwhile, the plunge cooling method reduces the crystallization of water due to a high cooling rate of ethane.

In the present study, human bone was used instead of that from an experimental animal. The orthodontic mini-implant was used as temporary skeletal anchorage in a patient and could be retrieved at the end of usage by unscrewing with a hand driver to obtain a sample with the proper thickness of attached bone on implant. A prosthetic implant would not be removable in this way. When using SEM-FIB to avoid chemical preprocessing of the samples, the interface between human bone and implant should be within 100 μm of the attached bone surface because the FIB cannot illuminate the interface if the interface is positioned too deeply. However, mechanical force could disrupt the osseointegration interface, and, consequently, it was not easy to find appropriate samples for observation. All of the samples were placed in saline solution and sent to the lab for cryofixation in ethane solution within 1 hour. All the ethane in the specimen was completely vaporized when the specimen was dried at room temperature; thus, it was believed that the sample was not affected by the ethane itself.

The possibility of chemical integration between bone and a Ti implant was suggested[17] based on evidence that implants with smooth surfaces also demonstrated osseointegration in an animal experimental model. Sul et al.[18] also asserted that chemical integration occurred by face and cortical bone. If there was true chemical integration, CaTiO compound should exist in the interface. In the present study, the presence of CaTiO compound was confirmed by the IVAS peak decomposition program, even though its exact distribution could not be verified. Previously, another study[2] also demonstrated the possible existence of CaTiO in the interface by STEM-EELS (scanning transmission electron microscope-Electron energy loss spectroscopy) analysis.

To date, activation of bone formation has been considered to be dependent on surface roughness or on the presence of particular proteins.[18] Figure 3 of this study showed that the interface between titanium and bone was characterized on one side by components of the implant (Ti, Al, and V) and on the other side by the components of bone (Ca, P, and C, as representative of proteins). However, at the site of the interface between bone and the implant, C was at very low levels, and most of the interface had implant metal components (Ti, Al, V) and bone mineral components (Ca, P). Since there was no carbon at the site of osseointegration, it meant that there were no proteins at the interface between the implant and bone. Therefore, osseointegration was not mediated by intermediary proteins. The scarcity of carbon at the interface suggested that the atomic mechanism of osseointegration was through direct mineral components of bone to titanium.

The nanostructure on the surface of an implant can increase the bond strength between bone and the implant. When APT is conducted, the sample is under a high electrical field for projecting atoms to the screen.[19] As a result of the difference in electric conductivity between bone and the metal implant, there is a high risk of fracture at the interface during APT operation. Breakage of the first sample occurred at 20 minutes, which might have been due to the weak integration of the bone and implant. However, the second sample remained intact until adequate observation of the sample was achieved, although partial fractures occurred in some areas. The difference in APT operating time between these samples may have been due to an integrated nanostructure at the interface between the implant and the bone tissue in the second sample. This nanostructure could have resulted in improved bond strength, allowing the sample to withstand the high electrical field in the APT analysis.

The overlapped peaks of ions could not be avoided because of the difficulty of identification by indexing; therefore, there was some imprecision in analysis at the interface, and the exact ionic distribution remained unclear. As the interface between human tissue and biomaterial is formed from various ions and amorphous materials,[18] the overlapped peaks were indeed limitations of APT analysis of the interface. However, the ionic reconfiguration of the interface was scrutinized with explicit consideration of these limitations.

It is important to consider that information regarding the identity, position, and chemical nature of atoms within a given material does not represent the whole composition of the material. The main objective of obtaining nanostructural information, in this case for the bone-tissue interface, was to gain insight into the relationship between the nanostructure and the properties and their functional features of osseointegration. SLA treatment of the implant surface contributed to formation of the surface nanostructure, allowing the calcium phosphates that diffuse into the interface to form tight contacts. Indeed, this area did not fracture during the APT analysis, which suggested that the nanostructure may contribute to the strong integration between the bone and the implant. Therefore, additional experimental studies, such as in vivo debonding strength tests in implants with various amounts of nanostructures, are required to determine the functional relationship between the current nanostructural observations and osseointegration.

## CONCLUSIONS

- Although the titanium implant–bone interface was extensively investigated, the exact mechanism of osseointegration remains unclear. APT by cryofixation was used for nanoscale resolution of the titanium-bone interface in a human patient. 1D profiling of each layer demonstrated high Ca and P concentrations in the bone, TiO in the interface, and Ti in the implant.
- This demonstration of an atom-sharing zone at the interface provides insights into the process of osseointegration.

## ACKNOWLEDGMENT

This work was supported by a National Research Foundation of Korea (NRF) grant funded by the Korean government (MSIP) (2012R1A5A2051384).

## REFERENCES

1. Brånemark P. Osseointegrated implants in the treatment of the edentulous jaw. *Scand J Plast Reconstr Surg Suppl*. 1977;16:1–132.
2. Kim JS, Kang SM, Seo KW, et al. Nanoscale bonding between human bone and titanium surfaces: osseohybridization. *BioMed Res Int*. 2015;2015.
3. Sundell G, Dahlin C, Andersson M, Thuvander M. The bone-implant interface of dental implants in humans on the atomic scale. *Acta Biomater*. 2017;48:445–450.
4. Kim SH, Lee SJ, Cho IS, Kim SK, Kim TW. Rotational resistance of surface-treated mini-implants. *Angle Orthod*. 2009;79:899–907.
5. Chung K, Kim SH, Kook YA. C-orthodontic microimplant for distalization of mandibular dentition in Class III correction. *Angle Orthod*. 2005;75:119–128.
6. Kim SH, Cho JH, Chung KR, Kook YA, Nelson G. Removal torque values of surface-treated mini-implants after loading. *Am J Orthod Dentofacial Orthop*. 2008;134:36–43.
7. Giavaresi G, Fini M, Cigada A, et al. Mechanical and histomorphometric evaluations of titanium implants with different surface treatments inserted in sheep cortical bone. *Biomaterials*. 2003;24:1583–1594.
8. Hong SB, Kusnoto B, Kim EJ, BeGole EA, Hwang HS, Lim HJ. Prognostic factors associated with the success rates of posterior orthodontic miniscrew implants: a subgroup meta-analysis. *Korean J Orthod*. 2016;46:111–126.
9. Palmquist A, Grandfield K, Norlindh B, Mattsson T, Brånemark R, Thomsen P. Bone–titanium oxide interface in humans revealed by transmission electron microscopy and electron tomography. *J R Soc Interface*. 2012;9(67):396–400.
10. Kulkarni M, Mazare A, Schmuki P, Iglič A. Biomaterial surface modification of titanium and titanium alloys for medical applications. *Nanomedicine*. One Central Press, Editors: Alexander Seifalian, Achala de Mel, Deepak M. Kalaskar, pp. 111–136, 2014.
11. Murai K, Takeshita F, Ayukawa Y, Kiyoshima T, Suetsugu T, Tanaka T. Light and electron microscopic studies of bone-titanium interface in the tibiae of young and mature rats. *J Biomed Mater Res*. 1996;30:523–533.
12. Karlsson J, Sundell G, Thuvander M, Andersson M. Atomically resolved tissue integration. *Nano Lett*. 2014;14:4220–4223.
13. Narayan K, Prosa TJ, Fu J, Kelly TF, Subramaniam S. Chemical mapping of mammalian cells by atom probe tomography. *J Struct Biol*. 2012;178:98–107.
14. Gordon LM, Tran L, Joester D. Atom probe tomography of apatites and bone-type mineralized tissues. *ACS Nano*. 2012;6:10667–10675.
15. Taborelli M, Jobin M, Francois P, et al. Influence of surface treatments developed for oral implants on the physical and biological properties of titanium. (I) Surface characterization. *Clin Oral Implants Res*. 1997;8:208–216.
16. Malm J, Giannaras D, Riehle MO, Gadegaard N, Sjövall P. Fixation and drying protocols for the preparation of cell samples for time-of-flight secondary ion mass spectrometry analysis. *Anal Chem*. 2009;81:7197–7205.
17. Takatsuka K, Yamamuro T, Nakamura T, Kokubo T. Bone-bonding behavior of titanium alloy evaluated mechanically with detaching failure load. *J Biomed Mater Res Part A*. 1995;29:157–163.
18. Sul YT, Kwon DH, Kang BS, Oh SJ, Johansson C. Experimental evidence for interfacial biochemical bonding in osseointegrated titanium implants. *Clin Oral Implants Res*. 2013;24:8–19.
19. Kelly TF, Larson DJ. Atom probe tomography 2012. *Annu Rev Mater Res*. 2012;42:1–31.